Environmental and Climate Technologies
2021, vol. 25, no. 1, pp. 931–943
https://doi.org/10.2478/rtuect-2021-0070
https://content.sciendo.com

Mechanical Properties of Alkali Activated Material Based on Red Clay and Silica Gel Precursor

Girts BUMANIS[1*], Danute VAICIUKYNIENE[2]

[1,2]*Faculty of Civil Engineering and Architecture, Kaunas University of Technology, Studentų St. 48, LT-51367 Kaunas, Lithuania*

***Abstract* –The search for alternative alumosilicates source for production of alkali activated materials (AAM) is intensively researched. Wide spread of natural materials such as clays and waste materials are one of potential alternatives. In this research AAM was made from local waste brick made of red clay and calcined low-carbonate illite clay precursor and its properties evaluated. Waste silica gel containing amorphous silica from fertilizer production plant was proposed as additional raw material. 6 M and 7 M NaOH alkali activation solutions were used to obtain AAM. Raw materials were characterized by X-ray diffraction, laser particle size analyser, DTA/TG. Raw illite clay was calcined at a temperature of 700 to 800 °C. Waste brick was ground similar as raw clay and powder was obtained. Replacement of red clay with silica gel from 2–50 wt.% in mixture composition was evaluated. Results indicate that the most effective activator was 6 M NaOH solution and AAM with strength up to 13 MPa was obtained. Ground brick had the highest strength results and compressive strength of AAM reached 25 MPa. Silica gel in small quantities had little effect of AAM strength while significant strength reduction was observed with the increase silica gel content. The efflorescence was observed for samples with silica gel.**

***Keywords* – Compressive strength; geopolymers; industrial by-product; precursor; technogenic silica gel**

1. INTRODUCTION

Alternative binder for Portland cement with similar mechanical performance and lower carbon footprint are researched around the world [1]. Up to now geopolymers or alkali activated materials (AAM) are one of most promising materials [2], [3]. Traditionally, AAM are synthesized from metakaolin or fly ash based precursors which now are associated with valuable raw and secondary raw material consumption [4]–[6]. However, research continues for alternative alumina and silica sources to obtain low cost alternative binders. There is a number of researches which focuses on obtaining AAM from different clay types. Up to now, the suitability of other clay based raw materials as precursors for AAM binders, such as mica, smectite or even interstratified illite-smectite has not been well researched [7]–[9]. The Baltic States such as Latvia and Lithuania are rich with red clay deposits and red clay valorization in production as an alternative binder seems to present opportunities. It has been reported that the red clays in Thailand have high potential to produce low-cost geopolymers [10]. Illite clay calcining temperature varies between 600–900 °C while the most cases select 800 °C [11], [12]. Some reports state that it has not yet been possible to synthesize meta-illite-smectite-based geopolymers of high strength (>20 MPa) without the addition of

* Corresponding author.
E-mail address: girts.bumanis@rtu.lv

cement additives [13]. Recent research, however, has proven that the border of 20 MPa has been passed. Illite clay has been valorized as a substitute of metakaolin in the synthesis of new geopolymeric materials and compressive strength reached 23 MPa, while hybrid system with 50 % metakaolin could reach 40 MPa [14]. Similar result was obtained by Ounissi *et al.* which reached strength of 25 MPa at the age of 7 days [11]. Calcined illite clay chemical treatment with an 8 M NaOH solution can also lead to the formation of the zeolites and sodium aluminium silicate hydrate [15]. The highest compressive strength was reached by heating the clay to 850 °C or 950 °C, but the dehydroxylation of such silicates are generally complete at lower temperatures (<800 °C, [16]), the precise reason why this higher temperature range produced metaclays with higher reactivity remained unclear [7].

The clay brick production industry is responsible for generating high amounts of solid wastes around the world from manufacture process failures, such as ineffective firing and issues related to product transportation and most of these products are based on red clay [8]. Besides, the necessity of clean alternatives to discard solid wastes, the civil construction industry has been demanding the development of better technological properties in new materials. Azevedo *et al.* have concluded that geopolymerization of bricks using the ceramic brick waste can be utilized in geopolymerization reactions as the metakaolin substitute and it was concluded that the method is feasible [8]. This means that brick manufacturers have brick waste which can be used as geopolymers precursors to produce high value products such as AAMs. Some problems are associated with the use of brick waste in the production of AAM. The amorphous SiO_2 and Al_2O_3 content in such brick waste tends to be low, there are reports that amorphous content in brick can be in range from 7.7–13.9 % for SiO_2 while Al_2O_3 from 9.6–12.9 %. The remaining main oxides are enclosed in crystalline phases [17], [18]. Ceramic precursors are characterized by a density of around 2.6 g/cm^3, d_{50} from 41–42 μm, $S_{g\ BET}$ 3.7–3.9 m^2/g. The density of brick powder precursor AAM in the range from 1600–1865 kg/m^3 could lead to compressive strength from 23–39 MPa [17].

Silica gel is proposed as another potential precursor of AAM. Silica gel is a by-product obtained from fertilizer production industry and up to now its application is limited. It is disposed in open stacks bringing environmental hazard concerns. Silica gel has high content of SiO_2 and therefor might be attractive for use in alkali activation process as silica source. 1 t of produced AlF_3 generates about 0.5 t of silica gel and up to now the use of the silica gel is limited due to the presence of fluoride compounds [9]. Fluoride compounds are hazardous because of its toxicity, irritating and health hazard properties. In building materials, they may negatively affect material properties as fluoride compounds retard the setting process and decrease the mechanical properties of hardened cement pastes and create aggressive environment for steel rebars [19], [20]. The effort of utilizing silica gel as precursor in AAM has been published by Borg *et al.*, which concluded that 25 % of silica gel add during calcination of clay was an optimal amount [9].

AAM as alternative binder for construction industry were evaluated. This research compares mechanical properties of AAM based on calcined raw red clay with ground waste brick precursors. An addition of silica gel was evaluated in the mixture composition of AAM. Different alkali activator solutions were tested.

2. Materials and Methods

2.1. Raw Materials

Thermally treated carbonate-free Illite clay (IC) from Liepa deposit in Latvia was used as a precursor in the alkali activation process. Calcined red brick waste was used as precursor

from the brick factory originated near the IC deposits. The appearance of the raw materials is given in Fig. 1. After drying at 105 °C raw IC and brick waste was milled to a powder with collision milling in a semi-industrial disintegrator. Differential thermal analysis / Thermogravimetric analysis (DTA/TG) was performed. The raw IC was heat treated from 700–800 °C with heating rate 5 °C/min and duration at maximum temperature was 4 h. Then the X-ray diffraction (XRD) and laser particle size distribution were determined.

In this investigation, silica gel waste obtained from a fertilizer production plant was used. The material was not treated before use. Freshly produced silica gel has a moisture between 80 wt.% and 100 wt.% and in this research water was not removed but included in mixture calculations. Commercially available Tianye Chemicals Ltd. (China) sodium hydroxide flakes with 99 % purity were used to prepare the alkali activation solution.

Fig. 1. Raw materials. Silica gel, unburned red clay before milling and red brick sand.

2.2. Testing Methods

The XRD analysis was performed using a *D8 Advance* diffractometer (Bruker AXS, Karlsruhe, Germany) operating at a tube voltage of 40 kV and tube current of 40 mA. The X-ray beam was filtered with 0.02 mm Ni filter to select the CuKα wavelength. The power X-ray diffraction patterns were identified with references available in the PDF-2 data base (PDF-2 International Centre for Diffraction Data, 12 Campus Boulevard Newtown Square, PA 19073-3273 USA).

The XRFA analyses of clay and silica gel waste were performed using a fluorescence spectrometer *S8 Tiger* (Bruker AXS, Karlsruhe, Germany) operating at the counter gas Helium 2 bar. The chemical elements of the materials were investigated with the *Bruker Quad 5040* energy-dispersive X-ray spectrometer (EDS) detector (123 eV). The microstructure of silica gel waste, red clay, calcined precursor, and alkali-activated calcined precursor were studied using *Veho Discovery DX-3* with magnification of 40x and 120x. A high-resolution scanning electron microscope *FEI Quanta 200 FEG* with a Schottky field emission gun (FEG) was used for the research.

The specific surface was measured using the semi-automatic Blaine instrument (TESTING Bluhm & Feuerherdt GmbH, 1.0290E) according to EN 196-6:2010 standard [19]. Tests of physical and mechanical properties of the AAM samples were performed on a *Zwick Z100* universal testing machine (according to LVS EN 12859:2011 and LVS EN 13279-1).

2.3. Sample Preparation

A number of series with AAMs were prepared using calcined red clay, ground brick and silica gel. Mixture composition of prepared AAMs are given in Table 1 and Table 2. The first batch of AAM samples were prepared with red clay treated at different temperatures from 700 to 800 °C and ground red brick as precursors. Precursor was activated with 6 or 7 M NaOH solutions as most common alkali-activation solution concentrations available in

literature (Table 1) [21], [22]. Alkali activator solution-solid precursor ratio (AAS/solid) was 0.6 for calcined clay and 0.43 for ground brick. Lower AAS/s ratio was associated with a coarser nature of ground brick precursor.

TABLE 1. MIXTURE COMPOSITION OF AAM MADE OF CALCINED RED CLAY, GROUND BRICK AND SILICA GEL AS PRECURSOR AND ACTIVATED WITH 6 M OR 7 M NAOH SOLUTION, % BY WEIGHT

Composition	6 M NaOH	7 M NaOH	Red clay	AAS/solid
700C/6M	60	–	100	0.60
800C/6M	60	–	100	0.60
Brick/6M	43	–	100	0.43
700C/7M	–	60	100	0.60
800C/7M	–	60	100	0.60
Brick/7M	–	43	100	0.43

The second part of the experiment included a partial replacement of ground brick with silica gel from 2 to 50 wt.% (Table 2). Silica gel was used in a natural state and extra water was included in calculations in AAS/solid ratio. The free moisture content in natural appearance silica gel may vary from 85–100 wt.%. The fine nature of silica gel increased AAS/soldi gradually as amount of silica gel increased. AAS/solid ratio increased from 0.43 to 0.86. Extra water was added to the system to ensure workability.

TABLE 2. MIXTURE COMPOSITION OF AAM WITH DIFFERENT GROUND BRICK AND SILICA GEL RATIOS ACTIVATED WITH 6 M NAOH, % BY WEIGHT

Composition	6 M NaOH	Brick	Silica gel	Silica gel+water	Water	AAS/solid
B100	43	100	–	–	–	0.43
B98/2	43	95	2.7	5	2	0.46
B95/5	43	95	5.5	10	4.675	0.47
B90/10	43	90	10	18.5	8.5	0.52
B80/20	43	80	20	37	17	0.60
B70/30	43	70	30	55.5	25.5	0.69
B60/40	43	60	40	74	34	0.77
B50/50	43	50	50	92.5	42.5	0.86

Samples were mixed with hand held electrical two shaft mixer. At first the raw solid raw materials were homogenized and then gradually poured in AAS. The mixture was mixed to obtain a homogenous mixture and cast in a silicon mold with dimensions of 20×20×20 mm. The molds were then covered with plastic film and put in a drying chamber at 80 °C for 24 h for curing. After 24h, the samples were demolded and early age strength was determined. The rest of the samples were divided in two parts where half of the remaining samples were cured at ambient room temperature at 22 °C, 50 % RH, another half was cured at moist environment 22 °C, 95 % RH. At the age of 28 days, the room temperature cured samples were tested while moist cured samples were conditioned in 22 °C, 50 % RH before tests at the age of 35 days.

3. RESULTS AND DISCUSSION

3.1. Description of Precursors

The chemical composition of IC is given in Table 3. Data indicate that red clay has a relatively low amount of Al_2O_3 (14.5 %) and high amount of SiO_2 (70.3 %). The high amount of Fe_2O_3 indicate that this clay is ferric aluminosilicate. A small amount of K_2O (4.0 %) and MgO (1.1 %) were also recorded. XRF analysis of silica gel indicates a high amount of SiO_2 (72.2 %) and Al_2O_3 (5.68 %) making such material highly attractive as precursor for production of AAM. Small traces of CaO and Fe_2O_3 were detected. High content of F was detected (21 %).

TABLE 3. XRF CHEMICAL COMPOSITION OF SILICA GEL AND RED CLAY FROM LODE, MASS, %

Compound	Silica gel	Red clay
Al_2O_3	5.7	14.5
SiO_2	72.2	70.3
CaO	0.4	0.3
TiO_2	–	0.9
Na_2O	–	0.1
K_2O	–	4.0
MgO	–	1.1
Fe_2O_3	0.7	5.4
F	21	–
Others	–	1.4
LOI, 1000°C	–	2.0
Total	100	100

The XRD analysis of calcined IC at 700 °C is given in Fig. 2.

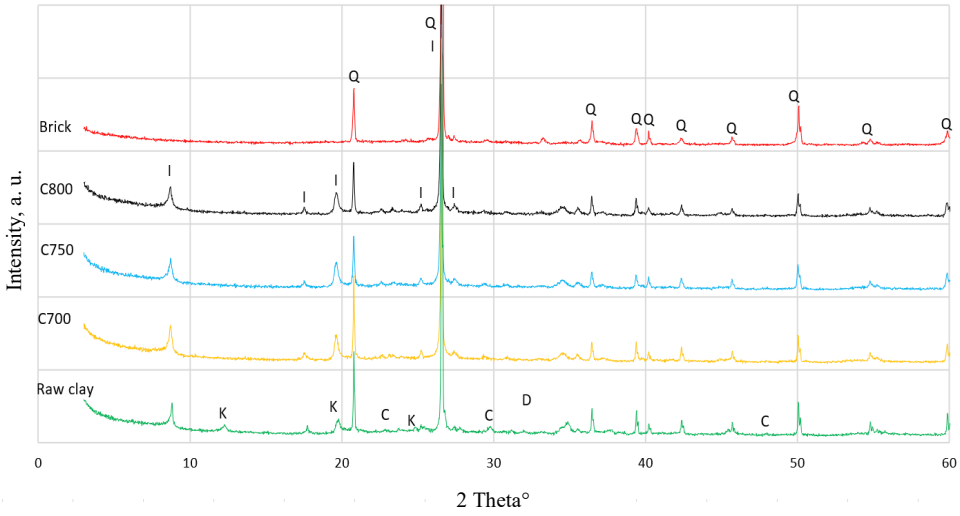

Fig. 2. The X-ray diffraction patterns of red brick waste, raw red clay and calcined red clay at different temperatures. Q – quartz SiO_2 (PDF-2 # 77-1060); I – illite (PDF-2 # 26-911); K – kaolinite (PDF-2 # 83-971); C – calcite $CaCO_3$ (PDF-2 # 83-578).

The main minerals were quartz SiO_2 (PDF-2 # 77-1060), illite (PDF-2 # 26-911), kaolinite (PDF-2 # 83-971) and calcite $CaCO_3$ (PDF-2 # 83-578). After calcination of clay kaolinite peak disappeared. For red clay brick illite peaks were also not detected. The XRD of silica gel is given in Fig. 3. The main crystalline compound in silica gel was aluminium fluoride hydrate. Also, amorphous part can be identified as a halo between 20° and 30° at 2 θ scale.

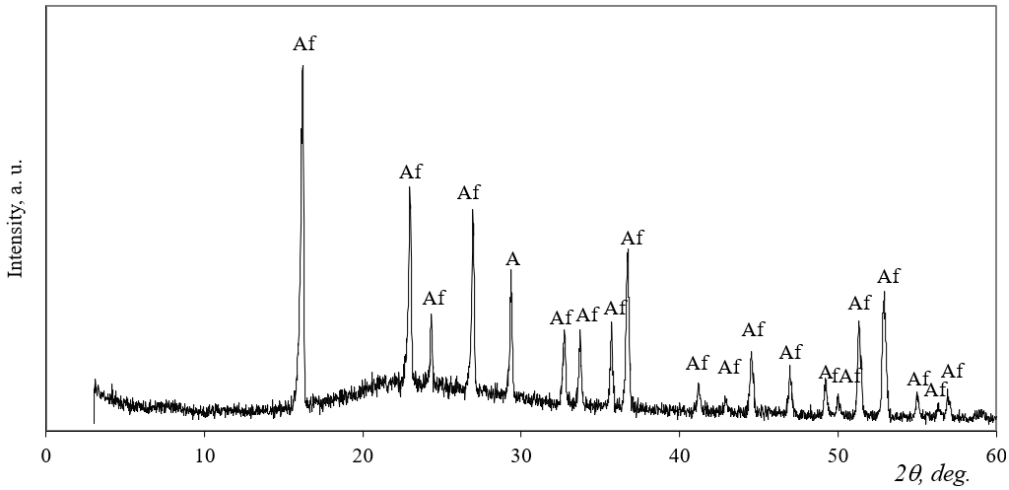

Fig. 3. The X-ray diffraction pattern of silica gel. Af – (PDF-2 # 35-827) aluminium fluoride hydrate ($AlF_3 \cdot 3.5H_2O$).

The DTA/TG analysis of raw clay is given in Fig. 4.

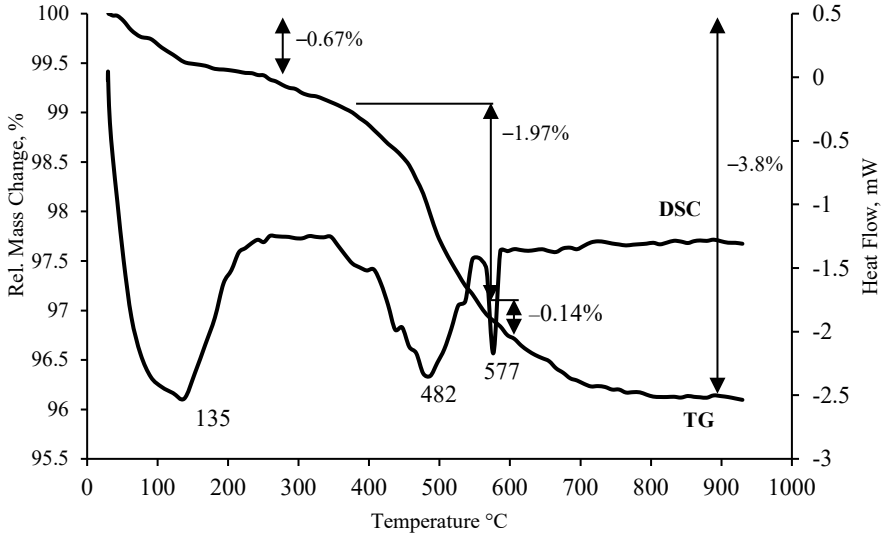

Fig. 4. DTA/TG analysis of raw clay.

The total mass change during the analysis was –3.8 %. Up to 214 °C mass change was –0.67 % and maximum peak was –2.524 mW at 135 °C and enthalpy –110.32 J/g. The next

temperature ranges with phase change detected was between 411 and 546 °C where mass change was –1.97 %, peak maximum was –2.363 mW at 482 °C and enthalpy was –57.65 J/g. High heat flow was detected between 573.4 and 580.9 °C where mass change was only –0.14 %, while peak maximum was –2.2 mW at 577 °C and enthalpy was –3.12 J/g. The first peak is associated with surface water desorption at low temperatures (35–214 °C). The dehydroxilation of clay occurred from 411–546 °C. Small mass loss due to the dehydroxylation of clay is associated with red clay small reactivity compared to kaolin clay, where mass loss may reach 8.5 % [23], [24]. A small endothermic peak starting at around 573 °C was associated with the allotropic transformation of quartz which also corresponds with the data from the XRD and literature [25].

The particle size distribution of ground red clay and precursors obtained from calcined red clay and brick is given in Table 4 and Fig. 5.

TABLE 4. PARTICLE SIZE AND CHARACTERISTICS OF MILLED CLAY MATERIALS AND SILICA GEL

	Raw clay	Calcination temperature, °C			Brick	Silica gel
		700	750	800		
Diameter at 10 %, µm	1.29	1.34	1.40	1.44	4.66	11.71
Diameter at 50 %, µm	5.50	6.02	7.19	8.26	52.65	66.39
Diameter at 90 %, µm	36.53	54.88	62.99	108.21	202.2	146.12
Mean d, µm	12.83	18.96	21.88	40.70	83.28	74.70
Density, g/cm^3	2.76	2.73	2.74	2.74	2.69	2.23
Specific surface, cm^2/g	4155	3925	3675	3475	1448	716

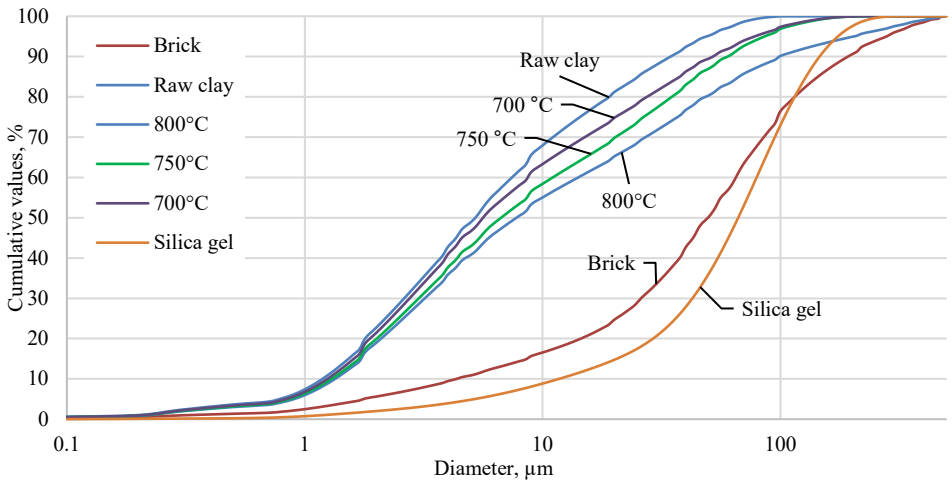

Fig. 5. Particle size distribution of ground clay treated at different temperatures, ground brick and silica gel.

Collision milling technique using disintegrator is described in previous paper [26]. The same grinding parameters was used both for raw clay and waste brick. Then raw clay was heated at temperatures of 700, 750 and 800 °C and particle size distribution was determined and compared. Results indicate that the finest state was for raw clay. d_{10} was 1.29 µm, d_{50} was 5.50 µm and d_{90} was 36.53 µm. Heating of ground raw clay powder gradually increased particle size and for red clay treated at 800 °C was characterized by d_{10} 1.44 µm, d_{50} 8.26 µm

and d_{90} 108.21 µm, respectively. Coarser particle size was for ground waste brick. d_{10} was 4.66 µm, d_{50} 52.65 µm and d_{90} 202.20 µm. This is associated with the hardness of burnt brick particles and higher energy is needed to ground material to finer state. The density of raw red clay was 2.76 g/cm^3 and slightly reduced after thermal treatment from 2.69 to 2.74 g/cm^3. Specific surface area reduced for clay treated at higher temperature which corresponds well with particle size distribution. Raw ground clay specific surface area was 4155 cm^2/g, it reduced from 3925 to 3475 cm^2/g for red clay treated at temperatures from 700–800 °C and for brick it was 1448 cm^2/g. The silica gel proved to be coarser than ground brick and it was characterized by d_{10} 11.71 µm, d_{50} 66.39 µm and d_{90} 146.12 µm. The specific surface area was 716 cm^2/g.

3.2. Properties of AAM

The macrostructure of prepared AAM are given in Fig. 6. AAM has typical red clay appearance as red to brown colour has remained also after alkali activation. Fig. 6(a) represents the macrostructure of 800C/6M while Fig. 6(b) – BR/6M. The nature of the precursors particle size is illustrated. As described before, it is evident that thermally-treated clay has finer particles compared to brick precursor. This appears also in the structure of AAM. Also entrapped air pores can be seen in both mixtures which are characteristic for such materials. Fig. 6(c) and 6(d) represent the macrostructure of AAM with silica gel (B60/40). White salts have fully covered the top surface of the samples. The efflorescence occurred during curing and drying of AAM. It was assumed that salts are associated with crystallization of silica gel and alkali activator solution, leading to formation of white salt crystals. This finding is supported by the literature, where efflorescence is associated with Na-based geopolymers.

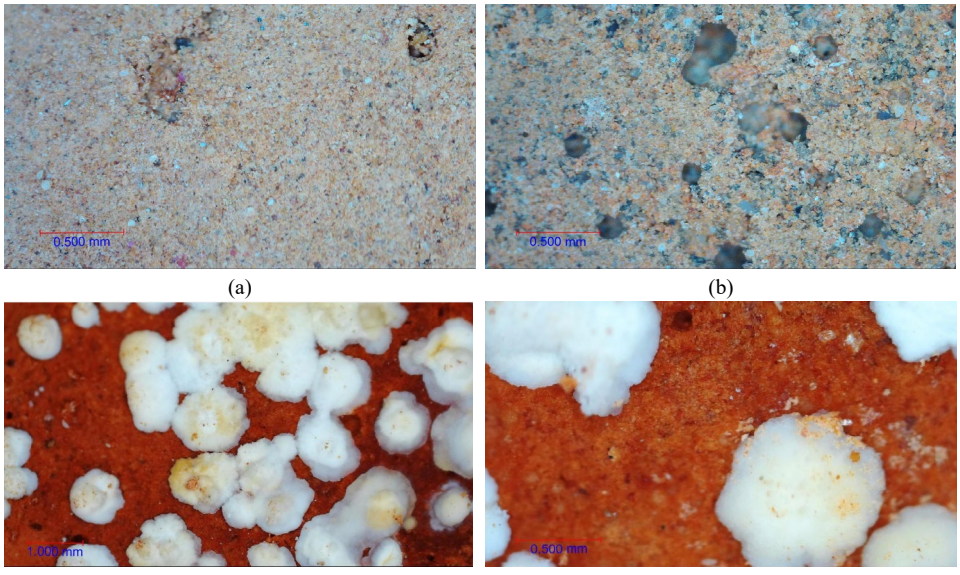

(a) (b)

(c) (d)

Fig. 6. AAM microstructure at 40× and 120× magnification: a) Calcined clay at 800 °C with 6 M NaOH activation solution; b) Ground brick precursor activated with 6 M NaOH; c) Ground brick (60 wt.%) and silica gel (40 wt.%) precursor activated with 6 M NaOH at 40x magnification; d) Ground brick (60 wt.%) and silica gel (40 wt.%) precursor activated with 6 M NaOH at 120× magnification.

Migration and carbonization of alkalis lead to white carbonate products [17], [28]. This is partially supported by the low mechanical strength results described in further sections. This phenomenon including XRD method will be investigated in more detail in further experiments.

The density of prepared AAM is given in Fig. 7 and Fig. 8. It is evident that density was slightly affected by the type of precursor and it was in a range from 1500–1770 kg/m^3. Slightly higher density was demonstrated for composition 700/6 M, while for 800/6 M and BR/6 M it was similar. For mixtures activated with 7 M NaOH AAS the density was lower at from 1225–1388 kg/m^3 for 700/7M and 800/7M while for BR/7M it was 1600 kg/m^3. AAM samples cured under moist conditions made of calcined clay and 7 M NaOH AAS decomposed during curing and was not able to be tested.

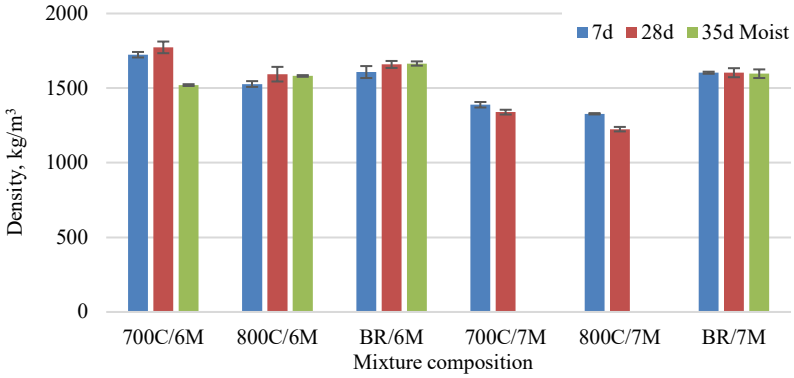

Fig. 7. Density of AAM with red clay precursors.

Incorporation of silica gel in mixture composition gradually reduced density of AAM (Fig. 7). It was associated mostly due to the fact that total volume of free water in AAM increased. Fine nature and naturally high moisture content in silica gel attracted even more water during alkali activation which also resulted in a decrease in density. By the increase of silica gel from 2 to 50 wt.%, the density decreased from 1665 to 850 kg/m^3. Together with the efflorescence phenomena, it reduced strength of AAM significantly.

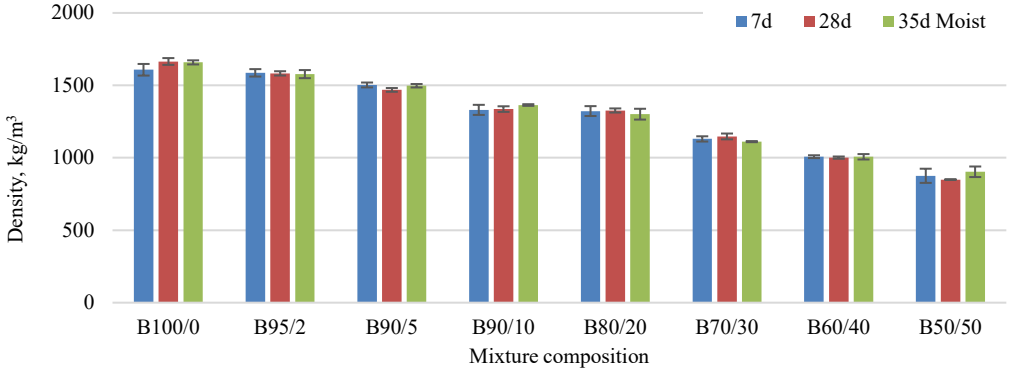

Fig. 8. Density of AAM with red brick and silica gel precursors.

The mechanical properties of prepared AAM is given in Fig. 9. Results proved that AAM strength increases over time and moist curing conditions were favourable in strength gain, if proper mixture composition was selected. Early age strength of AAM was from 4–5 MPa for red clay treated at 700 and 800 °C and activated with 6 M NaOH. It gradually increased to 6–9 MPa at the age of 28d and 11–16 MPa for moisture cured samples. Different results were obtained for AAM with same precursor but activated with 7 M AAS. The strength was marginally lower and reached only 2–3 MPa at the age of 28 d and moisture curing resulted in the sample bleeding and loss of integrity. The best mechanical performance was obtained for red brick precursor. The initial strength for AAM prepared with 6 M AAS was 14 MPa and remained the same at the age of 28 d, while for moist curing sample it reached 25 MPa. A similar tendency was also observed for AAM prepared with 7 M AAS. Even higher early strength was obtained at 7 d – 21 MPa, and moist curing increased the strength to 25 MPa.

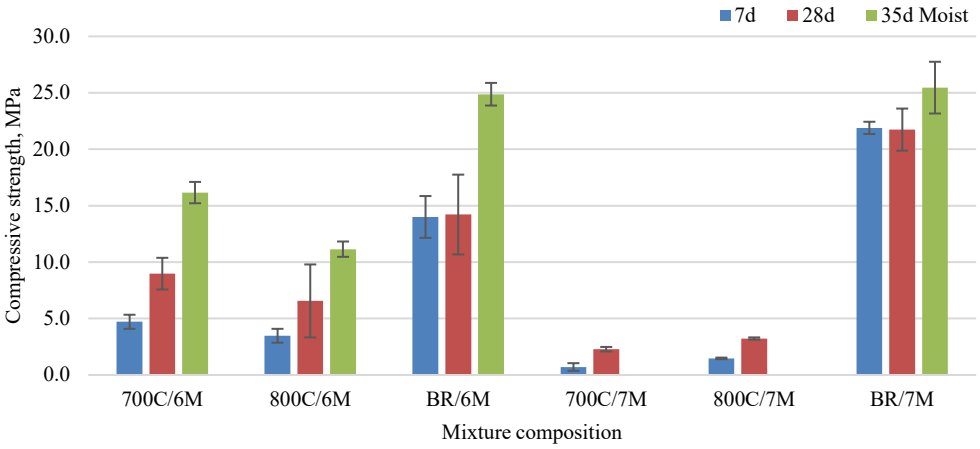

Fig. 9. Mechanical properties of red clay based AAM.

The effect of silica gel content in mixture composition on the strength of AAM is given in Fig. 10. It is clearly visible that the strenght gradually reduced as the content of silica gel increased. The small proportion of silica gel (2–5 wt.%) reduced strength slighly and it decreased from 22 MPa to 17 MPa for samples cured at moist conditions. Even for small content if silica gel caused visible traces of effluarescence which increased with the increasing amount of silica gel. 50 wt.% of silica gel in mixture composition reduced the strength 0.1–0.2 MPa. Results of obtained AAM in terms of strength correspond well to previous investigations. Borg *et al.* observed similar tendency as compressive strength decreased from 9 to 1 MPa as thermally treated (600 °C, 900 °C) silica gel addition was incorporated to AAM from 5 to 50 wt.% [9]. 6 M NaOH activation solution in combination with metakaolin obtained at 800 °C allowed to reach AAM with strength from 2 to 4 MPa while the increase of activation solution molarity increased materials compressive strength [29]. Similar tendency was observed in this research for ground brick precursor. As from the strength results can be observed, ground waste brick can be effectively used as precursor of AAM, allowing to avoid intended calcination procedure of raw clay powder. Also, silica gel has high content of SiO_2 needed for AAM preparation, even small addition to the mixture composition (2 wt.%) reduced strength while significant strength reduction was observed above 10 wt.% incorporation. As silica gel contains fluoride compound, they may act as Lewis acid in AMM mixture [30]. This could reduce Na content in activation

environment as NaF can form. Also, it was reported that incorporation of AlF_3 production waste increase porosity of AAM which could reduce the strength [31].

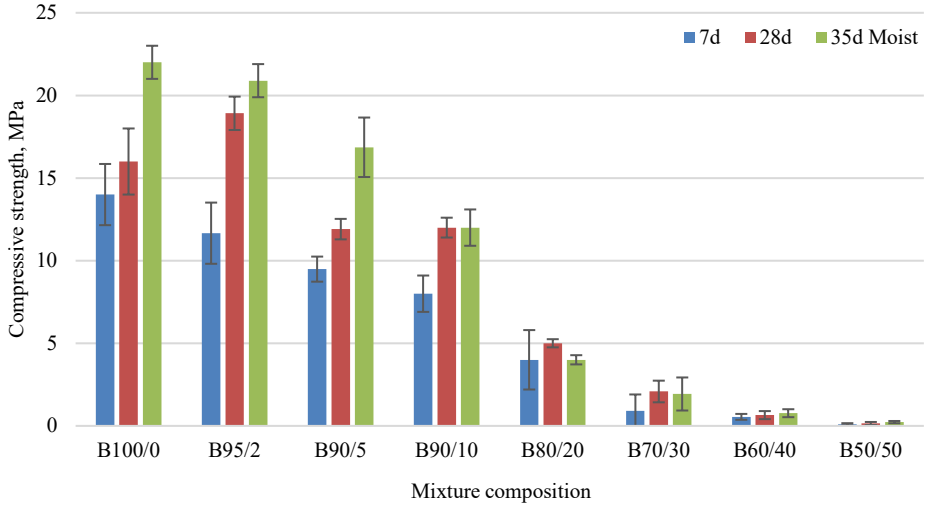

Fig. 10. Mixture composition of ground brick and different amount of silica gel AAM activated with 6 M NaOH.

4. Conclusion

The characteristic properties of low carbonate red illitic clay are associated with low Al_2O_3 content and partly crystalline SiO_2 which was detected both in XRD and DTA/TG. Despite a low reactive phase content, low-carbonate illite clay proved to be suitable for production of alkali activated materials (AAM). Alkali activated calcined low carbonate illite clay and waste brick reached a compressive strength up to 25 MPa, resulting in promising strength results for further development of sustainable materials. Such strength allows to use AAM as binder for mortars and concrete with similar properties to Portland cement-based materials. Waste silica gel with high Al_2O_3 and SiO_2 content proved to be unsuitable as precursor in present approach for production of AAM and the strength gradually decreased by increasing content of silica gel. Only 2 to 10 wt.% of silica gel was concluded to be suitable for incorporation in AAM as further increase of the material resulted in a dramatical strength decrease from 25 MPa to 0.1 MPa. Despite its coarse nature (fineness of 1448 cm^2/g), ground waste brick proved to be a promising precursor for production of AAM.

Acknowledgement

This research is/was funded by the European Social Fund under the No 09.3.3-LMT-K-712 “Development of Competences of Scientists, other Researchers and Students through Practical Research Activities” measure.

REFERENCES

[1] Podolsky Z., *et al.* State of the art on the application of waste materials in geopolymer concrete. *Case Stud. Constr. Mater.* 2021:15:e00637. https://doi.org/10.1016/j.cscm.2021.e00637
[2] Vaičiukynienė D., *et al.* Porous alkali-activated materials based on municipal solid waste incineration ash with addition of phosphogypsum powder. *Constr. Build. Mater.* 2021:301:123962. https://doi.org/10.1016/j.conbuildmat.2021.123962
[3] Bajpai R., *et al.* Environmental impact assessment of fly ash and silica fume based geopolymer concrete. *J. Clean. Prod.* 2020:254:120147. https://doi.org/10.1016/j.jclepro.2020.120147
[4] Vegere K., *et al.* Alkali-activated metakaolin as a zeolite-like binder for the production of adsorbents. *Inorganics* 2019:7(12):141. https://doi.org/10.3390/inorganics7120141
[5] Bocullo V., *et al.* The influence of the SiO_2/Na_2O ratio on the low calcium alkali activated binder based on fly ash. *Mater. Chem. Phys.* 2021:258:123846. https://doi.org/10.1016/j.matchemphys.2020.123846
[6] Gailitis R., *et al.* Long-Term Deformation Properties of a Carbon-Fiber-Reinforced Alkali-Activated Cement Composite. *Mech. Compos. Mater.* 2020:56(1):85–92. https://doi.org/10.1007/s11029-020-09862-w
[7] Dietel J., *et al.* The importance of specific surface area in the geopolymerization of heated illitic clay. *Appl. Clay Sci.* 2017:139:99–107. https://doi.org/10.1016/j.clay.2017.01.001
[8] Azevedo A. R. G., *et al.* Potential use of ceramic waste as precursor in the geopolymerization reaction for the production of ceramic roof tiles. *J. Build. Eng.* 2020:29:101156. https://doi.org/10.1016/j.jobe.2019.101156
[9] Borg R. P.. *et al.* Alkali-Activated Material Based on Red Clay and Silica Gel Waste. *W. Bio. Val.* 2020:11(6):2973–2982. https://doi.org/10.1007/s12649-018-00559-9
[10] Choeycharoen P., *et al.* Superior properties and structural analysis of geopolymer synthesized from red clay. *Chiang Mai J. Sci.* 2019:46(6):1234–1248.
[11] Ounissi C., *et al.* Potential use of Kebilian clay reserves (southern Tunisia) for the production of geopolymer materials. *Clay Miner.* 2020:55(2):101–111. https://doi.org/10.1180/clm.2020.14
[12] Mohammed S. Processing, effect and reactivity assessment of artificial pozzolans obtained from clays and clay wastes: A review. *Cons. Buil. Mat.* 2017:140:10–19. https://doi.org/10.1016/j.conbuildmat.2017.02.078
[13] Hu N., *et al.* The influence of alkali activator type, curing temperature and gibbsite on the geopolymerization of an interstratified illite-smectite rich clay from Friedland. *Appl. Clay Sci.* 2017:135:386–393. https://doi.org/10.1016/j.clay.2016.10.021
[14] Eliche-Quesada D., *et al.* Effects of an Illite Clay Substitution on Geopolymer Synthesis as an Alternative to Metakaolin. *J. Mater. Civ. Eng.* 2021:33(5):04021072. https://doi.org/10.1061/(ASCE)MT.1943-5533.0003690
[15] Sedmale G., *et al.* Application of differently treated illite and illite clay samples for the development of ceramics. *Appl. Clay Sci.* 2017:146:397–403. https://doi.org/10.1016/j.clay.2017.06.016
[16] Emmerich K. Thermal analysis in the characterization and processing of industrial minerals. *European Mineralogical Union Notes In Mineralogy* 2011:9(1):129–170. https://doi.org/10.1180/EMU-notes.9.5
[17] Keppert M., *et al.* Red-clay ceramic powders as geopolymer precursors: Consideration of amorphous portion and CaO content. *Appl. Clay Sci.* 2018:161:82–89. https://doi.org/10.1016/j.clay.2018.04.019
[18] Vitola L., *et al.* Low-calcium, porous, alkali-activated materials as novel pH stabilizers for water media. *Minerals* 2020:10(11):935. https://doi.org/10.3390/min10110935
[19] Vaičiukyniene D., *et al.* Utilization of by-product waste silica in concrete - based materials. *Mater. Res.* 2012:15(4):561–567. https://doi.org/10.1590/S1516-14392012005000082
[20] Rudelis V., *et al.* The prospective approach for the reduction of fluoride ions mobility in industrial waste by creating products of commercial value. *Sustain.* 2019:11(3):16–18. https://doi.org/10.3390/su11030634
[21] Rattanasak U., Chindaprasirt P. Influence of NaOH solution on the synthesis of fly ash geopolymer. *Miner. Eng.* 2009:22(12):1073–1078. https://doi.org/10.1016/j.mineng.2009.03.022
[22] Delgado-Plana P., *et al.* Effect of activating solution modulus on the synthesis of sustainable geopolymer binders using spent oil bleaching earths as precursor. *Sustain.* 2021:13(13):7501. https://doi.org/10.3390/su13137501
[23] Conconi M. S., *et al.* Thermal behavior (TG-DTA-TMA), sintering and properties of a kaolinitic clay from Buenos Aires Province, Argentina. *Ceramica* 2019:65(374):227–235. https://doi.org/10.1590/0366-69132019653742621
[24] Bumanis G., Bajare D., Korjakins A. Influence of the carbonate-free clay calcination temperature and curing conditions on the properties of alkali-activated mortar. *Proc. International Scientific Conference "Innovative Materials, Structures and Technologies"* 2014. https://doi.org/10.7250/iscconstrs.2014.04
[25] Ntah Z. L. E., *et al.* Characterization of some archaeological ceramics and clay samples from Zamala -Far-northern part of Cameroon (West Central Africa). *Ceramica* 2017:63(367):413–422.
[26] Bumanis G., Goljandin D., Bajare D. The properties of mineral additives obtained by collision milling in disintegrator. *Key Engineering Materials* 2017:721:327–331. https://doi.org/10.4028/www.scientific.net/KEM.721.327
[27] Zhang Z., *et al.* Efflorescence : A Critical Challenge for Geopolymer Applications? *Proc. Concr. Inst. Aust. Bienn. Natl. Conf.* 2013.
[28] Sen Lv X., *et al.* Inhibition of Efflorescence in Na-Based Geopolymer Inorganic Coating. *ACS Omega* 2020:5(24):14822–14830. https://doi.org/10.1021/acsomega.0c01919

[29] Bumanis G., Bajare D., Locs J. The effect of activator on the properties of low-calcium alkali-activated mortars. *Key Eng. Mater.* 2014:604:169–172. https://doi.org/10.4028/www.scientific.net/KEM.604.169

[30] Krahl T., Kemnitz E. Aluminium fluoride – the strongest solid Lewis acid: structure and reactivity. *Catal. Sci. Technol.* 2017:7(4):773–796. https://doi.org/10.1039/C6CY02369J

[31] Borg R. P., *et al.* Preliminary investigation of geopolymer binder from waste materials. *Rev. Rom. Mater. Rom. J. Mater.* 2017:47(3):370–378.